Development 138, 2223-2234 (2011) doi:10.1242/dev.059535

Cyclin E and CDK-2 regulate proliferative cell fate and cell cycle progression in the *C. elegans* germline

Paul M. Fox[1], Valarie E. Vought[2], Momoyo Hanazawa[1], Min-Ho Lee[3], Eleanor M. Maine[2] and Tim Schedl[1,*]

SUMMARY

The *C. elegans* germline provides an excellent model for analyzing the regulation of stem cell activity and the decision to differentiate and undergo meiotic development. The distal end of the adult hermaphrodite germline contains the proliferative zone, which includes a population of mitotically cycling cells and cells in meiotic S phase, followed by entry into meiotic prophase. The proliferative fate is specified by somatic distal tip cell (DTC) niche-germline GLP-1 Notch signaling through repression of the redundant GLD-1 and GLD-2 pathways that promote entry into meiosis. Here, we describe characteristics of the proliferative zone, including cell cycle kinetics and population dynamics, as well as the role of specific cell cycle factors in both cell cycle progression and the decision between the proliferative and meiotic cell fate. Mitotic cell cycle progression occurs rapidly, continuously, with little or no time spent in G1, and with cyclin E (CYE-1) levels and activity high throughout the cell cycle. In addition to driving mitotic cell cycle progression, CYE-1 and CDK-2 also play an important role in proliferative fate specification. Genetic analysis indicates that CYE-1/CDK-2 promotes the proliferative fate downstream or in parallel to the GLD-1 and GLD-2 pathways, and is important under conditions of reduced GLP-1 signaling, possibly corresponding to mitotically cycling proliferative zone cells that are displaced from the DTC niche. Furthermore, we find that GLP-1 signaling regulates a third pathway, in addition to the GLD-1 and GLD-2 pathways and also independent of CYE-1/CDK-2, to promote the proliferative fate/inhibit meiotic entry.

KEY WORDS: Germline, Cyclin E, Stem cell renewal, Cell cycle progression, Meiotic development, *C. elegans*

INTRODUCTION

Stem cells achieve self-renewal through both the execution of mitotic cell division and maintenance of stem cell fate. Different stem cell types display distinct patterns of self-renewal and differentiation. For example, hematopoetic stem cells divide infrequently compared with ES cells (Orford and Scadden, 2008). Different modes of stem cell proliferation may necessitate distinct mechanisms to regulate not only cell cycle progression but also developmental fate. An important goal in stem cell biology is to describe developmental and cellular processes of stem cells and to identify molecular mechanisms by which these processes are regulated.

The *C. elegans* hermaphrodite germline provides a model for studying stem cell biology. In adults, all germ cell stages from mitotic proliferation through meiotic prophase and gametogenesis are present in a linear array (Hansen and Schedl, 2006; Kimble and Crittenden, 2007). Germ cells divide mitotically in the distal-most part of the germline, termed the proliferative or mitotic zone (Fig. 1A). Proliferative zone cells, a steady-state population of ~230 cells, are defined by the absence of meiotic prophase markers and include stem cells, as well as cells that presumably have initiated steps toward differentiation (meiotic S-phase and possibly transit amplifying cells) (Hansen et al., 2004a; Crittenden et al., 2006; Maciejowski et al., 2006; Cinquin et al., 2010). Unlike some other stem cell systems, the switch from proliferation to meiosis appears not to involve asymmetric cell division (Crittenden et al., 2006). This switch is observed across several cell diameters termed the meiotic entry region, which is delineated by the position where the distal-most cell has entered meiotic prophase and the proximal-most proliferative cell has not yet entered meiosis (Hansen et al., 2004a). Within this region, various cellular processes, including mitotic cell division and both mitotic and meiotic S phase, occur in close proximity.

GLP-1 Notch signaling acts as a genetic switch for the proliferation versus meiotic entry decision (Austin and Kimble, 1987; Berry et al., 1997); constitutive GLP-1 activation causes all germ cells to have the proliferative fate and results in the formation of a germline tumor, whereas loss of GLP-1 activity results in premature meiotic entry of all germ cells. Premature meiotic entry occurs either temporally in early larval development in *glp-1*-null mutants, or spatially in the adult proliferative zone of *glp-1* temperature-sensitive hypomorphic mutants shifted to the restrictive temperature. Ligands for GLP-1, APX-1 and LAG-2 are expressed in the somatic niche distal tip cell (DTC), which contacts the very distal-most proliferative zone germ cells (Henderson et al., 1994; Nadarajan et al., 2009). In distal germ cells with presumably high GLP-1 signaling, downstream co-factors LAG-1 and SEL-8 are thought to cooperate with GLP-1 INTRA to induce transcription of genes that promote the proliferative fate (Christensen et al., 1996; Doyle et al., 2000; Petcherski and Kimble, 2000).

A major factor regulating the proliferative versus meiotic entry decision is GLD-1 level (Crittenden et al., 2002; Hansen et al., 2004b). High GLD-1 promotes entry into meiosis whereas low

[1]Department of Genetics, Washington University School of Medicine, St Louis, MO 63110, USA. [2]Department of Biology, Syracuse University, Syracuse, NY 13244, USA. [3]Department of Biological Sciences, University at Albany, Albany, NY 12222, USA.

*Author for correspondence (ts@genetics.wustl.edu)

Accepted 4 March 2011

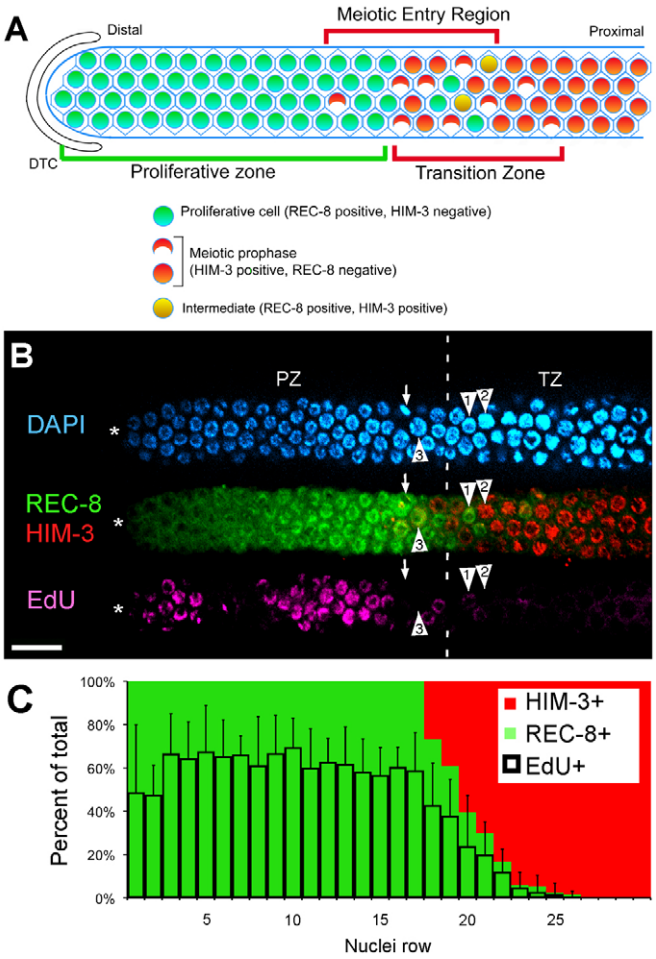

Fig. 1. S phase occurs equivalently throughout the proliferative zone. (**A**) Adult hermaphrodite proliferative zone contains ~230 cells defined by the presence of proliferative zone markers and the absence of meiotic prophase markers (e.g. REC-8 positive, HIM-3 negative). The meiotic entry region contains proliferative zone cells and cells that entered meiotic prophase (REC-8 negative, HIM-3 positive). The transition zone (TZ) marks the distal-proximal boundaries where crescent-shaped leptotene/zygotene nuclei are observed. The distal TZ boundary is the first row with multiple crescent shaped nuclei. (**B**) Confocal surface layer section of the distal region of a dissected adult hermaphrodite germline. Nuclei of proliferative zone cells are REC-8 positive (green); those in meiotic prophase are HIM-3 positive (red). Nuclei of S-phase (pink) cells are labeled with a <30-minute EdU-pulse. HIM-3 positive nuclei are almost exclusively EdU negative. Arrow indicates M-phase cells near the TZ. Arrowheads indicate adjacent TZ nuclei in distinct developmental stages: (1) EdU- and REC-8-positive nucleus (EdU signal dim), probably in meiotic S phase; (2) EdU-negative, HIM-3-positive nucleus in meiotic prophase; and (3) EdU negative, REC-8 positive, largely HIM-3-negative nucleus. (**C**) Cells in rows 1-30 were analyzed for three characteristics on a per-row basis: REC-8, HIM-3 and S phase (EdU incorporation after short pulse). Graph shows percentage of cells per row that are positive for each marker. The EdU-labeling pattern shown in B might suggest that there are two populations of S-phase cells. However, when many germlines were analyzed for EdU incorporation, ~60% of cells on average were in S phase. Scale bar: 20 μm. Error bars show s.d.

GLD-1 allows the proliferative fate (Hansen et al., 2004b). GLD-1, a cytoplasmic translational repressor, defines one of two major pathways that function redundantly to promote meiotic entry (Francis et al., 1995; Jones and Schedl, 1995; Hansen et al., 2004b). These pathways, called the GLD-1 and GLD-2 pathways, act genetically downstream of GLP-1 signaling (Kadyk and Kimble, 1998; Hansen et al., 2004a). Another component of the GLD-1 pathway is NOS-3 (Hansen et al., 2004a). The GLD-2 pathway includes the GLD-2 cytoplasmic poly(A) polymerase (Wang et al., 2002) and GLD-3, an RNA-binding protein (Eckmann et al., 2004). It remains unclear how the regulatory activities of these pathways specifically promote the meiotic cell fate.

Germline stem cells proliferate by progressing through the mitotic cell cycle whereas daughters that initiate meiosis must leave the mitotic cell cycle. In budding yeast, nutrient deprivation causes G1 cell cycle arrest and meiotic initiation (Honigberg and Purnapatre, 2003; Wittenberg and La Valle, 2003). Cell cycle regulators appear to play an important role in this switch, keeping the mitotic cell cycle and meiotic initiation mutually exclusive (Colomina et al., 1999). In animals, nutrient deprivation is not the signal for meiotic entry. Instead, nutrient deprivation can affect the rate of stem cell proliferation, at least in part through insulin signaling (Drummond-Barbosa and Spradling, 2001; Hsu et al., 2008; Michaelson et al., 2010), with meiotic entry controlled by developmental pathways (Crittenden et al., 2002; Hansen et al., 2004b; Matson et al., 2010). Nevertheless, in animals, control of the mitotic cell cycle and core cell cycle regulators is also likely to be important in the switch from proliferation to meiosis.

Further dissection of cell cycle behavior in the *C. elegans* proliferative zone may shed light on how these cells are regulated to achieve a proper balance between self-renewal and differentiation. We have investigated kinetic and regulatory features of mitotic cell cycle progression in proliferative cells in the adult hermaphrodite germline. Our results describe a previously unappreciated cell cycle structure wherein proliferative germ cells progress through the cell cycle without a noticeable G1 phase. We find that this rapid cell cycle is probably supported by constitutive CYE-1/CDK-2 activity, bypassing the need for upstream CDK-4/CYD-1 activity during G1. In addition, CYE-1 and CDK-2 promote the proliferative fate as RNAi depletion of *cye-1* or *cdk-2* in a *glp-1* partial loss-of-function mutant causes premature meiotic entry. Our results suggest that proliferative zone cells may, in part, coordinate cell cycle progression with maintenance of the proliferative cell fate through the common positive regulator CYE-1/CDK-2.

MATERIALS AND METHODS

Nematode maintenance and strains

Animals were propagated under standard conditions at 20°C unless noted otherwise. Strains used in this study were as follows: N2 Bristol (BS), wild type; N2 Bristol (JK), wild type; PD8488, *rrf-1(pk1417)*; BS3679, *rrf-1(pk1417); glp-1(bn18)*; BS3538, *rrf-1(pk1417); glp-1(ar202)*; BS4019, *prom-1(ok1140) unc-55(e405)*; BS673, *gld-1(q485)/hT2gfp*; BS3369, *gld-2(q497) gld-1(q485)/hT2gfp*; BS3392, *gld-2(q497) gld-1(q485)/hT2gfp; unc-32(e189) glp-1(q175)/hT2gfp*; BS3792, *gld-3(q730) nos-3(oz231)/mIn1::GFP*; BS5444, *gld-3(q730) nos-3(oz231)/mIn1::GFP; unc-32(e189) glp-1(q175)/hT2*; BS3855, *gld-1(q485)/ccIs4251 unc-13(e51); gld-3(q730)/mIn1::GFP*; BS5264, *gld-2(q497)/hT2; nos-3(oz231)*; BS5268, *gld-2(q497)/hT2; nos-3(oz231); unc-32(e189) glp-1(q175)/hT2*; BS4026, *gld-1(q485) prom-1(ok1140)/hT2gfp*; KM48, *cdk-4(gv3)/szT1*; KM123, *cdk-4(gv3)/szT1; Ex[PpPD95.67, CDK-4::GFP]*; BS1175, *cdk-4(gv3)/szT1; ozEx76[sur-5::dsred, CDK-4::GFP]*.

EdU time-course experiments

Plates seeded with MG1693 bacteria that incorporated 5-ethynyl-2′-deoxyuridine (EdU, Invitrogen) were prepared similar to BrdU-labeled bacteria plates (Ito and McGhee, 1987) except EdU was substituted for BrdU at 20 μM final concentration. Hermaphrodites were raised at 20°C, with some experiments repeated at 15°C and 25°C (see Fig. S1 in the supplementary material). Synchronized animals, 24 hours past mid-L4, were transferred by a pick from regular OP50-plates to EdU-labeled bacteria plates and immediately dissected (Jones et al., 1996) following labeling. For pulse-chase experiments, animals were transferred from EdU plates to OP50 plates. After crawling away from residual EdU-labeled bacteria on OP50-plates, animals were transferred to a fresh OP50-plate to minimize EdU-labeled bacterial carry over. Fixed germlines were first incubated with primary and secondary antibodies and 4′,6-diamidino-2-phenylindole (DAPI), followed by the EdU detection reaction using an EdU-labeling kit (Invitrogen). All time-course samples were analyzed using a PerkinElmer spinning disk confocal microscope and Volocity imaging software. EdU-positive nuclei (see Fig. S4 in the supplementary material) were scored throughout the proliferative zone by assaying multiple focal planes.

Immunohistochemistry

Germlines were dissected, fixed and stained essentially as described (Jones et al., 1996). Antibodies were as follows: rat anti-REC-8 (1:100) from Joseph Loidl (University of Vienna, Austria); rabbit anti-HIM-3 (1:100) from Monique Zetka (McGill University, Canada); rabbit anti-phospho-(Ser10)-Histone 3 (pH3) (1:400) from Upstate; guinea pig anti-SUN-1 S8-Pi (1:1000) from Verena Jantsch (University of Vienna, Austria); mouse anti-CYE-1 (1:10); and rabbit anti-pCDC-6 (1:50) from Edward Kipreos (University of Georgia, USA). Germlines were imaged either with a PerkinElmer spinning disk confocal microscope, and analyzed using Volocity software, or with a Zeiss compound microscope, and analyzed with Axiovision. Whole germline images were assembled using Adobe Photoshop and placed on a black background.

DNA quantification

Animals, 24 hours past mid-L4, were fed EdU-labeled bacteria for 30 minutes prior to dissection/fixation. Extruded germlines were stained with DAPI at a concentration of 100 ng/ml, and for pH3 and EdU as above. Three-dimensional germline images were recorded using a PerkinElmer spinning disk confocal microscope with *z*-stacks spaced every 0.3 microns. Volocity software was used to image nuclei in individual *z*-stacks, manually drawing a region of interest (ROI) encompassing a single nucleus to obtain a fluorescence value corresponding to the DAPI signal within that ROI. Fluorescence values from all *z*-stacks spanning a given nucleus were summed by obtaining a total fluorescence value. Background for each image was determined from the fluorescence value of empty space within the field of view and subtracted from the total fluorescence value. To compile data from multiple germlines, values were normalized to an average value for internal 4n controls (prophase, metaphase and meiotic nuclei) from their respective germline.

RNAi experiments

For RNAi, plasmids were obtained from OpenBiosystems (Rual et al., 2004), sequence verified and seeded on NGM plates as described previously (Lee et al., 2007). For all analysis of *cye-1* and additional cell cycle factors, unless noted otherwise, mid-L4 animals were placed on the RNAi plates for 48 hours, dissected and assessed for spatial premature meiotic entry or cell cycle arrest.

Hydroxyurea treatment

Hydroxyurea (HU) was added to seeded NGM plates to a final concentration of 250 μM. With L4/adults, a 5-hour HU-plate incubation was sufficient to block detectable germline EdU incorporation. Wild-type or *glp-1(bn18)* animals were incubated on HU-plates for up to 48 hours, yet for all time-points tested only cell cycle arrest, but not premature meiotic entry, was observed (Fig. 5D, data not shown).

RESULTS

Cell proliferation occurs throughout the proliferative zone

An initial picture of cell cycle and meiotic entry kinetics in the adult hermaphrodite has come from analysis of BrdU and injected fluorescent-nucleotide incorporation into distal germ cell nuclei (Crittenden et al., 2006; Jaramillo-Lambert et al., 2007). Here, we extend this analysis employing the nucleotide analog EdU (Salic and Mitchison, 2008), which is visualized without harsh fixatives, allowing co-staining for cell cycle and cell fate markers: M-phase marker phospho-(Ser10)-histone H3 (pH3), proliferative zone marker nucleoplasmic REC-8 (Hansen et al., 2004a) and meiotic prophase marker HIM-3, a chromosome axis protein (Zetka et al., 1999).

We first analyzed cell cycle progression in adult hermaphrodites by feeding animals a short EdU pulse (<30 minutes) (Fig. 1B). Nearly all cells that labeled with EdU were REC-8 positive and HIM-3 negative, and ~57% of proliferative zone cells (REC-8-positive) were in S phase. These and previous results confirm that cells undergoing mitotic and meiotic S phase are contained in the proliferative zone (Jaramillo-Lambert et al., 2007). To assess the frequency of cell proliferation across the distal-proximal axis, we scored the percent of EdU-positive cells per row. Consistent with previous analysis, cells throughout the proliferative zone appear to be cycling at equivalent frequencies (Fig. 1C) (Crittenden et al., 2006; Jaramillo-Lambert et al., 2007).

C. elegans germ cells progress through the cell cycle rapidly and continuously

We initially used pulse-chase analysis to investigate mitotic cell cycle length. Animals were fed EdU-labeled bacteria for 30 minutes and then transferred to label-free bacteria to chase EdU out of the germline (see Fig. S2 in the supplementary material). The ability to perform an effective pulse-chase experiment allowed marking a cohort of EdU-positive cells that were in S phase at the time of the pulse to obtain an estimate of total cell cycle length by following their progress through subsequent cell cycle phases. Specifically, we monitored EdU-positive cells as they passed through M phase (Fig. 2A). During an 8-hour timecourse, we observed two waves of EdU-positive cells moving through M phase, one from hours 2-5 and a second starting at hour 7. These waves indicate two successive cell divisions that can be experimentally verified. Indeed, by simultaneously monitoring an increase in total EdU-positive cells and the number of EdU-positive cells that initiated meiotic prophase (REC-8 negative and HIM-3 positive) throughout the time-course, we find strong evidence that all EdU-positive nuclei either undergo cell division (accounting for mitotic S phase) or initiate meiotic prophase (accounting for meiotic S phase) (Fig. 2B,C). Therefore, the total length of the cell cycle could be as short as 5 hours.

Germline mitotic cell cycle lacks a significant G1

We next examined the cell cycle structure by assessing the absolute and relative lengths of each cell cycle phase. We began by measuring the length of G2 using a second time-course experiment. Animals were continuously EdU labeled, starting at t=0, dissected at 30-minute intervals and stained for pH3 and EdU to determine the percentage of M-phase cells that were EdU positive (Fig. 2D). This experiment reveals the time required for a cell labeled with EdU in S phase to pass through G2 and enter M phase, becoming pH3 positive, providing an estimate of G2 length. According to our data, G2 ranged from 1.5 hours, when EdU-positive M-phase cells

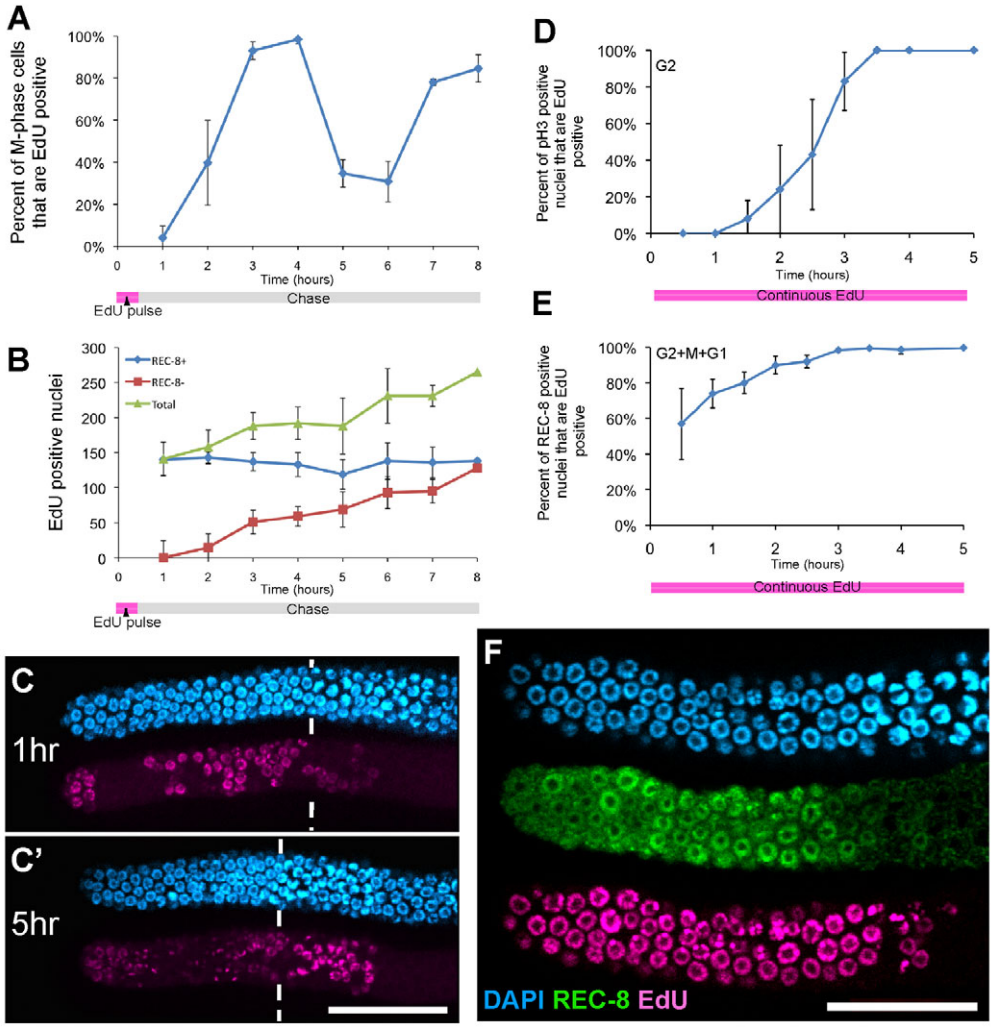

Fig. 2. Kinetic analysis of mitotic cell cycle progression in the germline. (**A**) Mitotic cell cycle length estimated from a pulse-chase experiment. Cohorts of EdU-pulsed (S-phase-labeled) cells were examined as they traversed the cell cycle passing M phase. Animals from pulse-chase experiments were dissected at 1-hour intervals and stained for EdU incorporation, pH3 and REC-8. The graph plots the percentage of cells in M phase (pH3-positive) containing EdU. (**B**) Plot of total number of EdU-positive nuclei from pulse-chase experiment scored as REC-8 positive or negative (averaged from two experiments). (**C**,**C'**) Representative images of germlines from 1 and 5 hours of the pulse-chase experiment show that by 5 hours there is a decrease in EdU signal intensity among distal nuclei due to cell division; proximal nuclei, which retain high EdU intensity, have entered meiosis. Vertical bars indicate the start of the transition zone. (**D-F**) Animals fed EdU continuously starting at *t*=0 were dissected at 30-minute intervals to obtain estimates of cell cycle phases. (D) Length of G2 estimated by analyzing the percent of cells in M phase (pH3-positive) that are EdU positive during the time course. (E) Length of G2+M+G1 estimated from the percentage of all REC-8-positive nuclei that are EdU positive. Averages from three experiments, with more than 10 germlines analyzed per time-point per experiment. (F) Representative germline after 3.5 hours of continuous EdU labeling showing all proliferative zone cells have incorporated EdU. Scale bars: 20 μm. Error bars show s.d.

were first detected, to 3.5 hours, when all M-phase cells were EdU positive. By 2.5 hours, ~50% of M-phase cells were EdU positive (Fig. 2D). Thus, the mitotic cell cycle in the germline has a median G2 length of ~2.5 hours with 1.5 and 3.5 hours as the minimum and maximum values, respectively.

Next, we measured the length of G2+M+G1 by determining the shortest time of continuous labeling required to mark all proliferative zone cells with EdU (Crittenden and Kimble, 2008). As the M-phase length is relatively short, this value allows us to infer the length of G1 through comparison with the length of G2. Fig. 2E shows that more than 99% of proliferative cells are EdU positive after 3.5 hours of continuous EdU feeding. This value of 3.5 hours for the maximum length of G2+M+G1 equals our value for the maximum length of G2 (Fig. 2D). This unexpected finding suggests that the lengths of G1 and M are very short relative to the length of G2. Consistent with this conclusion, we noticed that cells remaining EdU negative until hour 3.0 were enriched for M phase (see Fig. S3 in the supplementary material), indicating that cells return to S phase soon after completion of M phase. Finally, the fact that all cells in the proliferative zone incorporate EdU during a 3.5-hour pulse confirms previous reports that cells enter the cell cycle continuously and do not undergo significant periods of quiescence (Crittenden et al., 2006).

As an alternate approach to describe mitotic cell cycle structure, we estimated the proportion of proliferative zone cells in G1 by measuring the DNA content of DAPI-stained nuclei (Fig. 3). As histogram plots of DNA content among cells did not reveal obvious G1, S and G2 populations (Feng et al., 1999; Michaelson et al.,

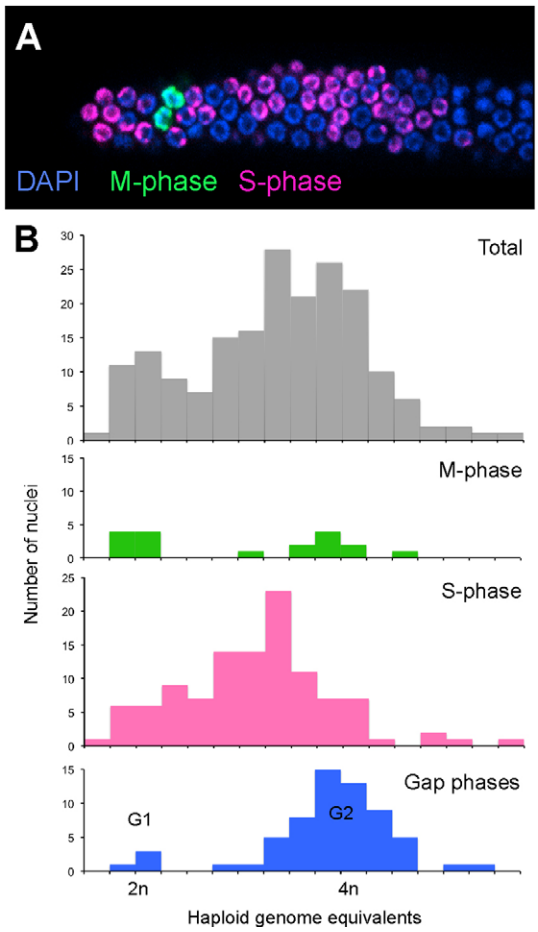

Fig. 3. G1 is largely absent from the germline mitotic cell cycle. (**A**) Animals were fed a 30-minute EdU pulse, immediately dissected and stained for EdU incorporation (S phase) and pH3 (M phase). (**B**) DNA content of proliferative cells determined by confocal microscopy; nuclei were scored for M phase, S phase and unlabeled Gap phase. Fluorescent intensity values corresponding to 2n and 4n DNA content (*x*-axis) were assessed by analyzing prophase and metaphase nuclei (4n) and individual daughters from anaphase/telophase (2n) as internal controls.

Table 1. Cell cycle summary

Proliferative zone cells*	231±23 (*n*=18)
S-phase cells†	133±20 (*n*=18)
S-phase index‡	57±5%
S-phase length§	3.5 hours
M-phase cells¶	5.2±2.3 (*n*=37)
M-phase index**	2%
G1 index††	2%
G2 index††	39%
G2 length‡‡	2.5 hours
Cell cycle length (based on G2 mean)§§	6.5 hours
Cell cycle length (based on G2+M+G1 maximum value)¶¶	8.0 hours

All measurements performed on N2 hermaphrodites 24 hours past L4 at 20°C.
*Average proliferative zone cells are determined by counting REC-8-positive cells (see Fig. 1).
†S phase is determined by pulsing animals with EdU for 30 minuets and counting total cells positive for EdU (see Fig. 1).
‡S phase index is determined by dividing number of S-phase-positive cells by the number of REC-8-positive cells.
§Length of S-phase is determined as 57% out of 6.4 hours.
¶M-phase is determined by counting pH3-positive nuclei.
**M-phase index is determined by dividng number of M-phase-positive cells by the number of REC-8-positive cells.
††G1 and G2 index is determined from DNA content analysis (see Fig. 3).
‡‡Mean G2 length is obtained from G2 timecourse experiment (see Fig. 2C).
§§Cell cycle length is extrapolated from the mean length of G2 and the G2 index.
¶¶Cell cycle length is extrapolated from 3.5 hours for G2+M+G1 (see Fig. 2D), which represents 43% of the total cell cycle.

2010) (Fig. 3B, gray bars), we used EdU and pH3 markers to identify cells in S phase and M phase, respectively. Phospho-H3-positive prophase and metaphase nuclei have 4n DNA content and fall into the right side of the histogram, whereas individual daughters from anaphase/telophase have 2n DNA content and fall into the left side (Fig. 3B, green bars). These 2n and 4n internal controls allow us to assign haploid DNA equivalents to corresponding DAPI fluorescence values for the remaining nuclei. As expected, most EdU-positive S-phase cells fall within a relatively even distribution between assigned 2n and 4n DNA content (Fig. 3B, pink bars). The remaining cells in Gap phase correspond to one of two distinct populations: a small population has 2n G1 DNA content, while a much larger population has 4n G2 DNA (Fig. 3B, blue bars). The frequency of 4n Gap phase outnumbers the frequency of 2n Gap phase ~20:1, indicating that G1 phase is very short compared with G2.

Our results allow us to model the mitotic cell cycle structure (Table 1). S phase, as determined by a short EdU-pulse (<30 minutes) labeling index, occupies ~57% of the total cell cycle [similar to ~50% (Crittenden et al., 2006) and 40-50% (Jaramillo-Lambert et al., 2007)], whereas M phase, as determined by the pH3 staining index, occupies 2% of the total cell cycle, consistent with previous results (Hansen et al., 2004a; Crittenden et al., 2006; Maciejowski et al., 2006). G1 and G2 occupy the remaining 41% of the cell cycle, during which cells are both pH3 and EdU negative. DNA content analysis indicates that 95% of these cells are in G2. Therefore, G2 represents ~39% (95% of 41%) and G1 represents ~2% (5% of 41%) of the total cell cycle.

Combining this cell cycle model with our kinetic measurements, we extrapolate a total cell cycle length of 8 hours. We reached this value using the method of Crittenden et al. (Crittenden et al., 2006), whereby the absolute and relative lengths of G2+M+G1 (3.5 hours and 43%, respectively) are combined. However, the assay for measuring the absolute length of G2+M+G1 provides only a maximum value (rather than median or average). Using 2.5 hours for the median length of G2 (as 39% of the total cell cycle) provides an estimate of 6.5 hours for the total cell cycle length, similar to the 5-hour estimate obtained from the pulse-chase experiment (Fig. 2). These estimates deviate significantly from 16-24 hours reported by Crittenden et al. (Crittenden et al., 2006) where the cell cycle estimate was derived from the measurement of G2+M+G1 (8-12 hours, 50% of the cell cycle). The discrepancy in estimates largely arises from a different measurement of the absolute length of G2+M+G1 (3.5 hours versus 8-12 hours); this difference cannot be explained by differences between the wild-type strains employed or the use of EdU versus BrdU (see Fig. S4 in the supplementary material). Experimentally, it is unclear why different results were obtained for this estimate.

As an additional assessment of cell cycle activity, we analyzed the output of the proliferative zone (number of cells entering meiotic prophase per unit time) by counting the flux of EdU-labeled cells out of the proliferative zone (see Fig. S5 in the supplementary material). We assume that the output of a proliferative zone of constant size is determined by the number of cells actively dividing and their average cell division rate. As some

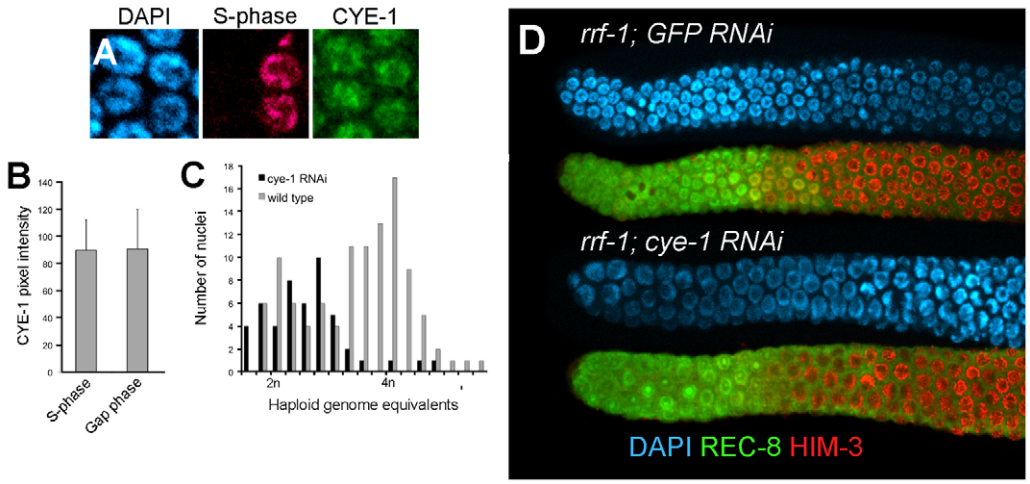

Fig. 4. CYE-1 levels are high throughout mitotic cell cycle progression and are required for passage through S phase. (**A**) CYE-1 is present at equal levels in S-phase and Gap-phase nuclei of proliferative zone cells. S-phase cells were identified by EdU-incorporation (pink) after a short pulse and CYE-1 (green) visualized by anti-CYE-1 staining. (**B**) Average fluorescence values were determined by assaying pixel intensity from confocal nuclear CYE-1 images. (**C**,**D**) *cye-1(RNAi)*, starting at mid-L4 for 48 hours. (C) DNA content of *cye-1(RNAi)* cell cycle arrested or wild-type control proliferative zone nuclei was determined by measuring DAPI fluorescent intensities from confocal image stacks. (D) A representative image shows that *cye-1(RNAi)*-depleted proliferative zone cells display an enlarged nuclear morphology relative to *GFP(RNAi)* controls. Error bars show s.d.

proliferative zone cells are in meiotic S phase, an average germline contains fewer than 230 actively cycling cells (Fig. 1). Experimentally, we observed an output of ~20 cells per hour (see Fig. S5 in the supplementary material). An average cell cycle length of 6.5 hours requires 130 actively cycling cells to achieve an output of 20 cells per hour, whereas an 8-hour cell cycle requires ~160 cells. (By contrast, a 16 hour cell cycle requires more than 350.) Based on these data, ~60-70% of proliferative zone cells are actively cycling, while ~30-40% are premeiotic.

Constant CYE-1/CDK-2 activity may drive rapid and continuous cell cycle progression

What regulatory features underlie this continuous and rapid cell cycle progression? In various cell types that lack G1, high cyclin E/CDK2 activity throughout the cell cycle is thought to drive entry into S phase independent of G1 factors, cyclin D and CDK4 (Orford and Scadden, 2008). Consistent with this, genetic mosaic analysis indicated that *cdk-4* is not required for cell cycle progression in the germline (see Fig. S6 in the supplementary material). Given a lack of both G1 and a requirement for CDK-4, we asked whether CYE-1 level is also high throughout the germline mitotic cell cycle. As previously reported, CYE-1 is found in nuclei throughout the proliferative zone (Brodigan et al., 2003; Biedermann et al., 2009) (see below). To investigate whether CYE-1 levels fluctuate according to cell cycle stage, we compared levels of CYE-1 in S-phase and non-S-phase (predominantly G2 with some M) cells. CYE-1 levels appeared constant throughout the cell cycle (Fig. 4A,B). In addition, we analyzed the abundance of phospho-CDC-6, a potential CYA-1/CDK-2 substrate that is, at least in part, dependent on CYE-1/CDK-2 activity (Kim et al., 2007). Nucleolar localized phospho-CDC-6 is present in all CYE-1-positive cells and is *cye-1* dependent but not *cdk-1* dependent (see Fig. S7 in the supplementary material). The phospho-CDC-6 staining thus suggests that CYE-1/CDK-2 activity is constant throughout the mitotic cell cycle throughout the proliferative zone, and is downregulated, along with CYE-1 levels, as germ cells enter meiotic prophase.

Although CDK-4 is not required for germline cell cycle progression, depletion of CYE-1 or CDK-2 causes cell cycle arrest (Fay and Han, 2000). When *rrf-1* mutants, which lack RNAi in the soma (Sijen et al., 2001), are treated with *cye-1* or *cdk-2 RNAi*, proliferative zone cells display an abnormal/enlarged nuclear morphology typical of cell cycle arrest and a reduction in proliferative zone cell number (Fig. 4D; see Fig. S8 in the supplementary material; data not shown). Consistent with these factors specifically functioning to promote progression into S phase, most of the arrested proliferative cells in *cye-1(RNAi)* treated germlines contained ~2n DNA content (Fig. 4C). Therefore, high CYE-1/CDK-2 activity may allow proliferative germ cells to bypass G1 by promoting progression into S phase.

CYE-1/CDK-2 promote the proliferative fate

CYE-1 could act to promote the proliferative fate, in addition to promoting cell cycle progression, with the prediction that depletion of CYE-1 or CDK-2 would cause proliferative cells to prematurely enter meiosis. As depletion of CYE-1 or CDK-2 leads to cell cycle arrest (Fig. 4C,D), which may mask meiotic entry, we asked whether RNAi depletion could promote meiotic entry of proliferative cells in a sensitized genetic background containing the *glp-1(bn18)* hypomorphic mutation (Qiao et al., 1995). We depleted CYE-1 by RNAi from *glp-1(bn18)* L4 animals, at the permissive temperature, in parallel with control *gfp(RNAi)* (Fig. 5). After 48 hours of RNAi treatment, no cells with the proliferative fate were evident in *glp-1(bn18); cye-1(RNAi)* germlines: meiotic cells extended to the distal end, a phenotype indicating spatial premature meiotic entry. This loss of proliferative cells due to increased meiotic entry indicates that CYE-1 plays an important role in regulating the decision to proliferate versus enter meiosis.

To address whether this premature meiotic entry phenotype is specific to *cye-1* or whether general loss of cell cycle function also promotes premature meiotic entry, we performed an RNAi screen for enhancement of *glp-1(bn18)* with a panel of cell cycle factors, as well as a set of GLD-1 mRNA targets that is enriched for cell cycle genes. Cell cycle arrest was observed for multiple cell cycle

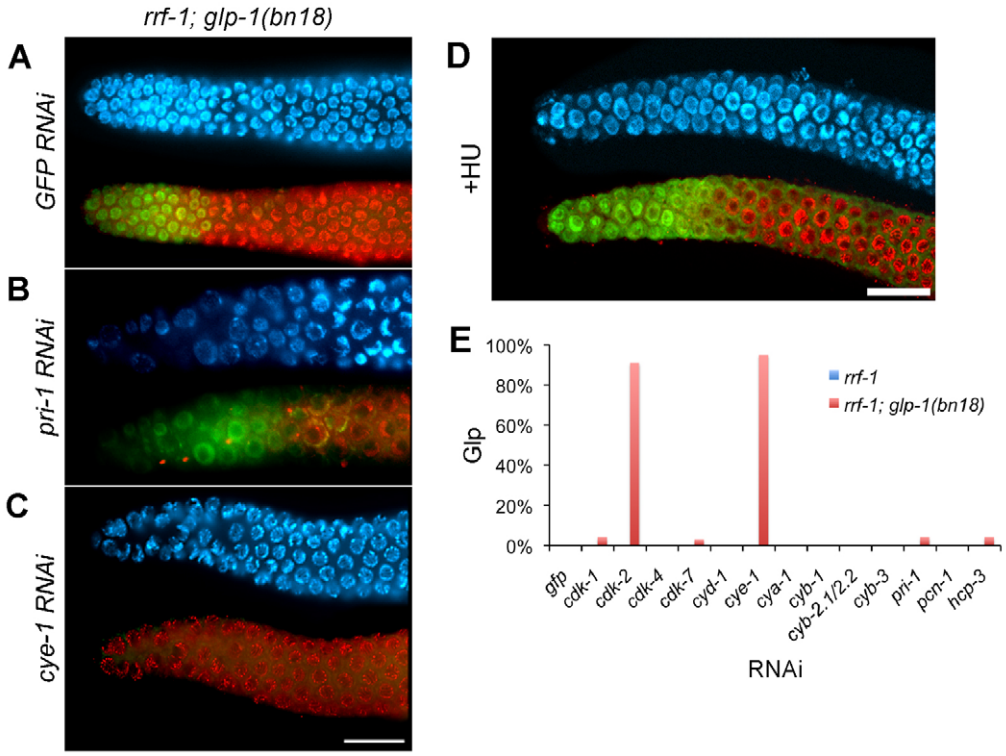

Fig. 5. CYE-1/CDK-2 promote the proliferative fate of germ cells. *glp-1(bn18)* provided a sensitized genetic background for monitoring premature meiotic entry. *glp-1(bn18)* mid-L4 hermaphrodites were fed RNAi bacteria or treated with hydroxyurea (HU) at 20°C and examined 48 hours later. (**A-D**) Proliferative cells, REC-8 positive (green); meiotic prophase cells, HIM-3 positive (red). (B,D,E) *pri-1(RNAi)*, which encodes the D subunit of DNA polymerase α-primase, or HU treatment illustrate the enlarged nuclei cell cycle arrest phenotype when most cell cycle factors were depleted by RNAi. (C) By contrast, depletion of *cye-1* or *cdk-2* in *glp-1(bn18)* resulted in a complete loss of the proliferative zone due to premature meiotic entry (Glp in E) (also see Fig. S8 in the supplementary material). (**E**) The percentage of animals scored Glp (premature meiotic entry) after 48 hours of RNAi. Scale bars: 20 μm.

factors, as well as following hydroxyurea treatment (a DNA synthesis inhibitor), whereas only *cye-1* and *cdk-2* RNAi enhanced the *glp-1(bn18)* premature meiotic entry phenotype (Fig. 5B-E; see Fig. S8 in the supplementary material; data not shown). Thus, a general loss of cell cycle function does not cause premature meiotic entry in *glp-1(bn18)*. Instead, the ability of *cye-1* and *cdk-2* to promote the proliferative fate is not likely to be a general cell cycle property but rather a function specific to these factors.

cye-1/*cdk-2* is epistatic to known meiotic entry regulatory pathways

We next asked where CYE-1 and CDK-2 act relative to the currently described genetic pathway for regulation of the proliferative versus meiotic cell fate decision. GLP-1 Notch signaling promotes the proliferative fate. The redundant GLD-1 and GLD-2 pathways act downstream of GLP-1 to promote meiotic entry; simultaneous loss of both pathways causes a defect in meiotic entry that leads to germline overproliferation and prevention of gamete production (Austin and Kimble, 1987; Kadyk and Kimble, 1998; Hansen et al., 2004a). We asked whether CYE-1 or CDK-2 depletion could promote meiotic entry independent of the activity of the GLD-1 and GLD-2 pathways. Thus, we performed *cye-1(RNAi)* or *cdk-2(RNAi)* in a series of double mutants containing putative null alleles of one gene in the GLD-1 pathway and another gene in the GLD-2 pathway (Table 2), asking whether loss of CYE-1 or CDK-2 would cause ectopic proliferative cells to enter meiosis. As previously shown, when germlines were mutated in both the GLD-1 and GLD-2 pathways, germlines display ectopic proliferative cells with some or no evidence of meiotic entry depending on the genes used, based on HIM-3 and pSUN-1 (an additional marker for initiation of meiotic prophase) (Penkner et al., 2009) staining (Fig. 6A; see Fig. S9 in the supplementary material). However, upon RNAi-mediated depletion of CYE-1 or CDK-2 for 48 hours, we observed many germ cells entering meiosis. As a control, when we depleted CDK-1 by RNAi from germlines lacking the GLD-1 and GLD-2 pathways, we observed cell cycle arrest but did not observe increased entry into meiosis, as determined by REC-8, HIM-3 and pSUN-1 staining (Table 2, data not shown). Therefore, loss of CYE-1 or CDK-2 can promote meiotic entry independent of the activity of either the GLD-1 or GLD-2 pathway. We conclude that CYE-1/CDK-2 promotes the proliferative fate downstream of or in parallel to the GLD-1 and GLD-2 pathways.

In these mutants, although meiotic entry occurred throughout much of the germline following *cye-1* and *cdk-2* RNAi, we never observed meiotic entry in the distal-most cells (Fig. 6; see Fig. S9 in the supplementary material). These cells correspond to the proliferative zone in wild-type, where DTC expressed LAG-2 and APX-1 mediates activation of GLP-1 signaling. Although it is possible that there is significant residual CYE-1/CDK-2 activity in the distal germline following *cye-1* RNAi, we think this is unlikely as CYE-1 was not detected by antibody staining in either the distal germline or proximal germline (data not shown). Instead, we hypothesized that GLP-1 activity, restricted to these distal proliferative cells, acts independently of CYE-1/CDK-2 to promote the proliferative fate. As the GLD-1 and GLD-2 pathways are genetically downstream of GLP-1 signaling, *gld-1gld-2* pathway; *glp-1* null triple mutants are tumorous (Kadyk and Kimble, 1998, Hansen et al., 2004a). Therefore, we asked whether *cye-1(RNAi)* could cause distal germ cells to enter meiosis in a series of *gld-1gld-2* pathway; *glp-1* triple mutants. Although *gld-1 gld-2* pathway; *glp-1* mutants remain tumorous when treated with *gfp(RNAi)*, we observed widespread meiotic entry in the adult germlines after 48 hours of *cye-1(RNAi)* (Table 2, Fig. 6B; see Fig. S9 in the supplementary material). Importantly, we observed meiotic entry in the distal-most cells, in contrast to the absence of meiotic entry in the distal-most cells in the *gld-1gld-2* pathway mutant; *cye-1(RNAi)* germlines. Therefore, GLP-1 can apparently act independently of

Table 2. Loss of *cye-1* suppresses germline tumors by promoting meiotic entry

Genotype	RNAi	Percentage of germlines with meiotic entry	Extent of meiotic entry†	Percent meiotic entry within distal 10 cell diameters	Average distance to first meiotic cell§	*n*
Wild type		100%	NA	0%	20	31
glp-1(ar202gf) 25°C	*GFP*	100%	**	0%	NA	21
glp-1(ar202gf) 25°C	*cye-1*	100%	**	0%	NA	27
gld-2(q497) gld-1(q485)	*GFP*	100%	***	0%	15	24
gld-2(q497) gld-1(q485) ‡	*cye-1*	100%	***	3%	13	28
gld-2(q497) gld-1(q485) ‡	*cdk-2*	100%	***	0%	15	28
gld-2(q497) gld-1(q485); glp-1(q175)	*GFP*	85%	**	12%	NA	41
gld-2(q497) gld-1(q485); glp-1(q175)	*cye-1*	100%	***	91%	2	22
gld-2(q497) gld-1(q485); glp-1(q175)	*cdk-2*	100%	***	32%	NA	34
gld-2(q497) gld-1(q485); glp-1(q175)	*cdk-1*	100%	**	0%	NA	19
gld-3(q730) nos-3(oz231)	*GFP*	0%	*	0%	NA	32
gld-3(q730) nos-3(oz231)	*cye-1*	100%	***	0%	21	25
gld-3(q730) nos-3(oz231)	*cdk-2*	88%	***	5%	14	18
gld-3(q730) nos-3(oz231)	*cdk-1*	0%	*	0%	NA	24
gld-3(q730) nos-3(oz231); glp-1(q175)	*GFP*	0%	*	0%	NA	23
gld-3(q730) nos-3(oz231); glp-1(q175)	*cye-1*	100%	***	75%	6	20
gld-3(q730) nos-3(oz231); glp-1(q175)	*cdk-2*	81%	***	55%	NA	22
gld-2(q497); nos-3(oz231); glp-1(q175)	*GFP*	100%	**	4%	17	23
gld-2(q497); nos-3(oz231); glp-1(q175)	*cye-1*	100%	***	90%	2	20
gld-1(q485); gld-3(q730)	*GFP*	93%	**	0%	NA	30
gld-1(q485); gld-3(q730)	*cye-1*	100%	***	10%	13	20
gld-1(q485); gld-3(q730)	*cdk-2*	100%	***	0%	NA	27

†Extent of meiotic entry is scored by counting the number of nuclei rows that contain cells in meiotic prophase as assayed by HIM-3 and pSUN-1 staining: *less than 5 cell diameters of meiotic entry; **5-30 cell diameters; ***more than 30 cell diameters.
‡*gld-2 gld-1* mutants show a qualitative increase in meiotic entry following *cye-1 (RNAi)* and *cdk-2 (RNAi)* (see Fig. S9 in the supplementary material).
§In mutant strains assigned 'NA'; the first meiotic cell did not occur in a reproducible position near the distal end of the gonad.

CYE-1/CDK-2 to promote the proliferative fate. Furthermore, GLP-1 signaling must have an additional activity besides regulating the GLD-1 and GLD-2 pathways because, as assessed by *cye-1(RNAi)*, GLP-1 can promote the proliferative fate/inhibit meiotic entry even in the absence of their activity. This result also sheds light on our initial finding that *cye-1(RNAi)* or *cdk-2(RNAi)* in wild type causes proliferative cells to undergo cell cycle arrest but not premature meiotic entry (Fig. 4D; see Fig. S8 in the supplementary material). By contrast, we observed premature meiotic entry in a sensitized background with decreased GLP-1 activity. Thus, loss of CYE-1/CDK-2 only causes meiotic entry when GLP-1 signaling is reduced, as presumably occurs when germ cells in the proliferative zone move away from the influence of the DTC.

CYE-1 is targeted for degradation upon entry into meiosis

CYE-1 remains high throughout the mitotic cell cycle, but its level sharply decreases as germ cells enter meiosis. GLP-1 signaling, however, is not necessary for CYE-1 accumulation as CYE-1 accumulates in proliferative cells of *gld-1 gld-2* pathway; *glp-1* null

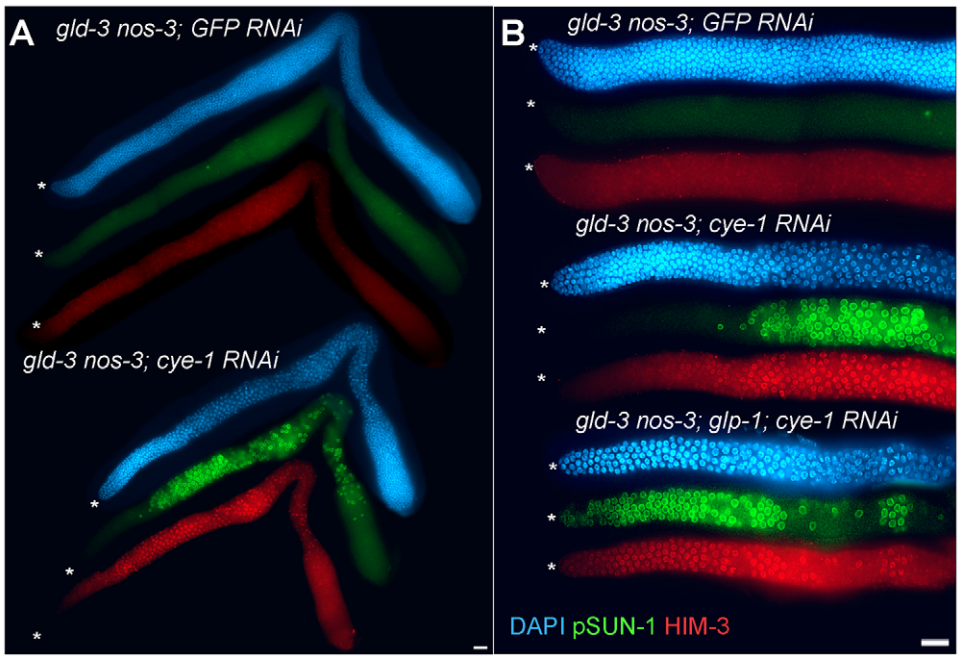

Fig. 6. CYE-1 is epistatic to the GLD-1 and GLD-2 pathways, and acts in parallel to GLP-1. (**A**) *gld-3(q730)nos-3(oz231)* null double mutants eliminate the function of both the GLD-1 and GLD-2 pathways, displaying a complete germline tumorous phenotype. Knockdown of CYE-1 by RNAi 'suppresses' the tumorous phenotype by causing proliferative cells to switch to meiotic development [HIM-3-positive (red) and pSUN-1-positive (green) nuclear staining]. Meiotic entry is observed throughout the germline except in the distal region corresponding to the vicinity where the proliferative zone is in wild type. (**B**) *gld-3(q730)nos-3(oz231); glp-1(q175)* null triple mutants have a tumorous germline. Here, *cye-1(RNAi)* in a *gld-3(q730)nos-3(oz231); glp-1(q175)* triple mutant causes germ cells at all positions, including distal, to enter meiosis. Asterisks mark the distal end. Scale bars: 20 μm.

triple mutants (see Fig. S10 in the supplementary material). Recently, it has been reported that GLD-1 binds and represses *cye-1* mRNA during the pachytene stage of meiotic prophase, suggesting that GLD-1 could be responsible for repression of CYE-1 upon entry into meiotic prophase (Biedermann et al., 2009). However, we found that the initial downregulation of CYE-1 remains intact in *gld-1*-null mutants; thus, a redundant mechanism may play a role in mediating CYE-1 repression in this region (see Fig. S11A,B in the supplementary material). To investigate whether CYE-1 is targeted for degradation upon meiotic entry, we analyzed CYE-1 in germlines depleted of candidate ubiquitin ligase factors. This analysis implicated three components of an SCF ubiquitin ligase, as required for CYE-1 repression: CUL-1 (Kipreos et al., 1996), SKR-1/-2 (Nayak et al., 2002) and PROM-1 F-box-like (Jantsch et al., 2007) (see Fig. S11C in the supplementary material; data not shown). In *prom-1* mutants, for example, CYE-1 decreases gradually after entry into meiosis, in contrast to the immediate repression in wild type. Thus, a PROM-1 dependent pathway may act together with GLD-1 to repress CYE-1 expression. To examine this, we analyzed *gld-1prom-1* double mutants and found that CYE-1 remained high throughout the germline (see Fig. S11D in the supplementary material). Therefore, GLD-1 may act in parallel with an SCF^{prom-1} ubiquitin ligase to repress and maintain low CYE-1 upon entry into meiotic prophase. Importantly, even in the presence of ectopic CYE-1, germ cells still enter meiosis in both *prom-1* single mutants and *gld-1prom-1* double mutants. Therefore, although CYE-1 is necessary to maintain the proliferative fate in certain instances, CYE-1 alone is not sufficient to promote the proliferative fate. Additionally, the combined activities of the GLD-1 and GLD-2 pathways are not necessary for downregulation of CYE-1 as germ cells enter meiosis. In *gld-2(q497)gld-1(q485)* mutant tumors, some germ cells enter meiosis (Hansen et al., 2004a). CYE-1 levels are downregulated in these meiotic germ cells (see Fig. S10 in the supplementary material; data not shown).

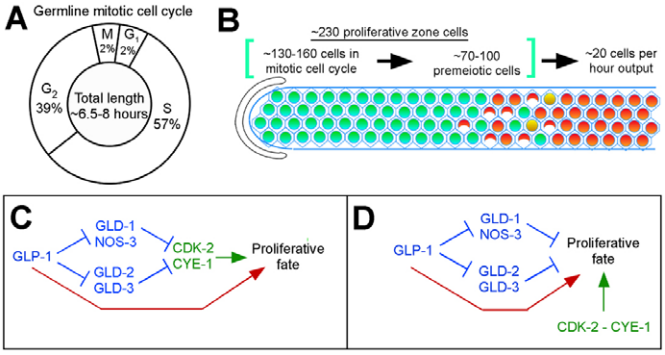

Fig. 7. Summary and model. (**A**) The mitotic cell cycle in the adult hermaphrodite germline lacks a significant G1 phase. S phase, as demonstrated here and by others, occupies the largest part of the cell cycle. G2 also comprises a significant part of the cell cycle. This model is consistent with regulatory characteristics and marker accumulation. (**B**) Our data combine to describe how proliferation in the germline is balanced by production of cells that enter meiosis. Proliferating germ cells undergo cell division on average once every 6.5-8.0 hours, which is balanced by ~20 cells entering meiosis per hour. This rate of cell production predicts ~130-160 cells (~60-70%) of the proliferative zone is undergoing mitotic cell cycle progression. This leaves an additional ~70-100 premeiotic cells that are not engaged in mitotic cell cycle progression. (**C**,**D**) Interactions among CYE-1/CDK-2, GLP-1 and the GLD-1 and GLD-2 pathways are consistent with at least two genetic models. Previous work indicates that the GLD-1 and GLD-2 pathways lie downstream of GLP-1. (C,D) CYE-1/CDK-2 (green) may lie downstream of the GLD-1 and GLD-2 pathways (C) or act in parallel (D). In addition and relevant to both models, our data indicate that GLP-1 activity (red) also promotes the proliferative fate/inhibits meiotic development by a mechanism independent of the GLD-1 and GLD-2 pathways, as well as CYE-1/CDK-2.

DISCUSSION

Cell cycle progression in the *C. elegans* germline

Proliferating germ cells in the adult hermaphrodite display three important kinetic characteristics: (1) continuous (Crittenden et al., 2006; Jaramillo-Lambert et al., 2007) and (2) rapid cell cycle progression, and (3) a cell cycle structure where the G1 phase is highly abbreviated or absent. Our results indicate that the average cell cycle length under standard laboratory conditions is ~6.5-8 hours. This work also determined the length of individual phases of the cell cycle (Fig. 7A) and leads to a description of the proliferative zone in terms of the number of mitotically cycling and premeiotic cells contained within the population (Fig. 7B).

Additional observations on regulatory features of the germline mitotic cell cycle correlate well with the cell cycle kinetics. CDK-4, a cyclin-dependent kinase required for cell cycle progression in larval somatic cells with a significant G1 phase (Park and Krause, 1999), is not required for cell cycle progression in the adult germline. In addition, CYE-1 accumulation – and activity as assessed by phospho-CDC-6 – is found throughout the germline mitotic cell cycle in contrast to its canonical periodic expression in somatic cells. High levels of CYE-1 may drive germ cells through the cell cycle without an appreciable G1 or a requirement for the G1 factor CDK-4. High levels of CYE-1 are also observed in other rapidly dividing cells that lack a significant G1 phase, including mouse embryonic stem cells (Stead et al., 2002) and early *Drosophila* and *Xenopus* embryos (Richardson et al., 1993; Rempel et al., 1995). Importantly in *Drosophila*, the male germline stem cell/cystoblast daughter lacks a detectable G1 phase under normal conditions (Yukiko Yamashita, personal communication), and the female germline stem cell has a short G1 with high cyclin E in G2 and M phase (Hsu et al., 2008). Thus, an atypical cell cycle structure with a short or no G1 and high cyclin E levels may be common in germline stem cell systems.

Role of CYE-1/CDK-2 in promoting the proliferative fate

Our finding that CYE-1/CDK-2 regulates cell fate adds to a growing body of evidence supporting this role, including previous examples in *Drosophila* (Berger et al., 2005; Wang and Kalderon, 2009), *C. elegans* (Fujita et al., 2007) and mouse embryonic stem cells (Neganova et al., 2009). In the *Drosophila* ovary, similar to what we observe in the *C. elegans* germline, decreased cyclin E causes premature meiotic entry during cystocyte transit amplification (Lilly and Spradling, 1996). Therefore, cyclin E/CDK-2 may be broadly important for promoting the proliferative fate/inhibiting meiotic entry, although it is unclear whether the *C. elegans* germline contains transit-amplifying cells.

How might CYE-1/CDK-2 promote the proliferative fate in the *C. elegans* germline? The DTC niche signals GLP-1 in distal germ cells to promote the proliferative fate. Although the spatial distribution of GLP-1 signaling activity is not known, the DTC surrounds the ~30 distal-most germ cells (Crittenden et al., 2006); therefore, signaling levels are probably highest in these cells.

GLP-1 signaling presumably decreases as the remaining ~100-130 mitotically cycling cells (Fig. 7B) move proximally through the proliferative zone. *cye-1* and *cdk-2* RNAi caused premature meiotic entry under conditions where GLP-1 signaling was compromised, but did not appear to prevent the proliferative fate when there was high GLP-1 activity. One model to explain these results is that the function of CYE-1/CDK-2 in promoting the proliferative fate is most important in cells with reduced GLP-1 signaling, which are those residing proximal to the DTC niche. An alternative model is that CYE-1/CDK-2 promotes the proliferative fate throughout the proliferative zone, but because of redundant pathways, this function is only revealed when GLP-1 signaling is compromised. Prior work has shown that genetic redundancy is pervasive in the *C. elegans* proliferation versus meiosis decision (Hansen and Schedl, 2006). Consistent with either model, CYE-1/CDK-2 may promote the proliferative fate by regulating cell cycle structure per se. For example, mouse ES cells may maintain their pluripotent and self-renewing potential by limiting the time spent in G1 phase, when differentiation-inducing factors might act upon them (Orford and Scadden, 2008). Also consistent with either model, CYE-1/CDK-2 may promote the proliferative fate through phosphorylation-mediated regulation of non-cell cycle proteins that control the proliferative and/or meiotic fate. Regardless, periodic CYE-1 levels may be undesirable, leading to unstable maintenance of the proliferative fate or proliferative zone size.

How do we relate the short/no G1 phase and high CYE-1 to the decision to enter meiosis? In budding yeast, nutrient deprivation causes cell cycle arrest and entry into meiosis in the G1 phase (Honigberg and Purnapatre, 2003), while in the mouse fetal ovary, loss of the meiosis promoting gene *Stra8* leads to germ cells arrested with a 2n DNA content (Baltus et al., 2006). These and other results suggest that the decision to enter meiosis may generally occur prior to meiotic S phase. In the adult hermaphrodite, we observe little/no G1 phase and no evidence of a lengthening G1 in the proximal half of the proliferative zone that might be indicative of preparation for switching to meiotic S phase. As only ~20 scattered proximal cells enter meiosis in a 1-hour period, it is possible that the appearance of, or a small lengthening of, G1 phase may have been missed. If so, such a G1 alteration would not be occurring through changes in CYE-1 level or activity. We currently lack markers to distinguish mitotic from meiotic S phase and our markers for meiotic entry assess initiation of early meiotic prophase (leptotene). Thus, the switch from mitotic cycling to meiotic S phase is only thus far observed on a population level (Fig. 7B). Current results do not distinguish whether the decision to enter meiosis occurs immediately prior to meiotic S phase or at another time.

Cyclin E/CDK-2 activity is often regulated via cyclin E levels. In the adult hermaphrodite, CYE-1 levels and activity are high throughout proliferative zone cells, falling as they enter meiotic prophase. In *Drosophila*, cyclin E levels also fall as germ cells enter meiotic prophase, in large part due to SCF-mediated protein degradation (Doronkin et al., 2003; Narbonne-Reveau and Lilly, 2009). However, the precipitous decrease in cyclin E levels as cells enter meiotic prophase, in *C. elegans* and *Drosophila*, is presumably not the trigger for entry into meiosis because it occurs after meiotic S phase. How, then, do proximal proliferative zone cells enter meiosis notwithstanding high CYE-1? Downregulation of CYE-1/CDK-2 activity appears not to be the mechanism for switching from mitotic to meiotic S phase as CYE-1 levels and activity are high throughout the proliferative zone. Instead, we favor a model where meiotic entry is triggered by other factors, such as the rise in GLD-1, the spatial control of which appears not to be regulated by *cye-1* and *cdk-2* (data not shown). This possibility is consistent with our finding that the presence of ectopic CYE-1 in the transition zone, through SCF ubiquitin ligase depletion, is not sufficient to promote the proliferative fate. Although CYE-1/CDK-2 activity alone does not determine proliferative versus meiotic cell fate, our results nevertheless indicate that CYE-1/CDK-2 contributes to promoting the proliferative fate and may serve as one of various signaling mechanisms that integrate cell fate decisions and proliferative zone dynamics.

Analysis of genetic interactions among CYE-1, GLP-1 and the GLD-1 and GLD-2 pathways reveals two important findings. First, depletion of CYE-1 or CDK-2 promotes meiotic entry independent of the activity of the GLD-1 and GLD-2 pathways. This indicates that CYE-1/CDK-2 acts downstream of (Fig. 7C) or in parallel to (Fig. 7D) the GLD-1 and GLD-2 pathways. Intriguingly, *cye-1* mRNA is a known target of GLD-1 (Biedermann et al., 2009), suggesting CYE-1 may be a true downstream factor in this pathway, in combination with SCF-mediated protein degradation. However, as CYE-1 is downregulated after meiotic S phase, this control may be distinct from the meiotic entry decision and instead be important for meiotic prophase progression (Francis et al., 1995; Biedermann et al., 2009). Therefore, we favor the possibility that CYE-1/CDK-2 acts in parallel to the GLD-1 and GLD-2 pathways. Second, GLP-1 can act independent of CYE-1/CDK-2 to promote the proliferative fate: GLP-1 retains the ability to promote the proliferative fate despite RNAi knockdown of CYE-1 and CDK-2 in wild-type and in *gld-1*, *gld-2* pathway double mutants (see Results). These findings suggest that GLP-1 also provides some activity in parallel to the GLD-1 and GLD-2 pathways and CYE-1/CDK-2 (Fig. 7C,D). Previous work suggested that there may be a third pathway, in addition to the GLD-1 and GLD-1 pathways, acting downstream of GLP-1 to promote proliferation/inhibit meiotic entry (Hansen et al., 2004a; Maine et al., 2004; Vought et al., 2005); however, these studies employed only a limited number of *gld-1*, *gld-2* pathway double mutant combinations where there is concern that GLD-2 pathway function is not fully eliminated (Mantina et al., 2009; Kerins et al., 2010). Here, we used all *gld-1*, *gld-2* pathway double mutant combinations, providing strong evidence that there is a third pathway, in addition to the GLD-1 and GLD-2 pathways, which is regulated by GLP-1 to control entry into meiosis.

Acknowledgements
We thank Sarah Crittenden for advice, discussions and the JK Bristol N2 strain; Siqun Xu for microinjections; and Maria Mercedes for assistance with the mosaic analysis. We thank Drs Hansen, Drummond-Barbosa, Arur, Engebrecht, Hubbard, Kipreos, Krause, Lilly, Seydoux and Yamashida for discussions and comments on the manuscript. We thank WormBase and the Caenorhabditis Genetics Center. This study was supported by NIH GM63310 to T.S. and NSF #IBN0077172 to E.M. Deposited in PMC for release after 12 months.

Competing interests statement
The authors declare no competing financial interests.

Supplementary material
Supplementary material for this article is available at
http://dev.biologists.org/lookup/suppl/doi:10.1242/dev.059535/-/DC1

References
Austin, J. and Kimble, J. (1987). glp-1 is required in the germ line for regulation of the decision between mitosis and meiosis in C. elegans. *Cell* **51**, 589-599.
Baltus, A. E., Menke, D. B., Hu, Y. C., Goodheart, M. L., Carpenter, A. E., de Rooij, D. G. and Page, D. C. (2006). In germ cells of mouse embryonic ovaries,

the decision to enter meiosis precedes premeiotic DNA replication. *Nat. Genet.* **38**, 1430-1434.
Berger, C., Pallavi, S. K., Prasad, M., Shashidhara, L. S. and Technau, G. M. (2005). A critical role for cyclin E in cell fate determination in the central nervous system of Drosophila melanogaster. *Nat. Cell Biol.* **7**, 56-62.
Berry, L. W., Westlund, B. and Schedl, T. (1997). Germ-line tumor formation caused by activation of glp-1, a Caenorhabditis elegans member of the Notch family of receptors. *Development* **124**, 925-936.
Biedermann, B., Wright, J., Senften, M., Kalchhauser, I., Sarathy, G., Lee, M. H. and Ciosk, R. (2009). Translational repression of cyclin E prevents precocious mitosis and embryonic gene activation during C. elegans meiosis. *Dev. Cell* **17**, 355-364.
Brodigan, T. M., Liu, J., Park, M., Kipreos, E. T. and Krause, M. (2003). Cyclin E expression during development in Caenorhabditis elegans. *Dev. Biol.* **254**, 102-115.
Christensen, S., Kodoyianni, V., Bosenberg, M., Friedman, L. and Kimble, J. (1996). lag-1, a gene required for lin-12 and glp-1 signaling in Caenorhabditis elegans, is homologous to human CBF1 and Drosophila Su(H). *Development* **122**, 1373-1383.
Cinquin, O., Crittenden, S. L., Morgan, D. E. and Kimble, J. (2010). Progression from a stem cell-like state to early differentiation in the C. elegans germ line. *Proc. Natl. Acad. Sci. USA* **107**, 2048-2053.
Colomina, N., Gari, E., Gallego, C., Herrero, E. and Aldea, M. (1999). G1 cyclins block the Ime1 pathway to make mitosis and meiosis incompatible in budding yeast. *EMBO J.* **18**, 320-329.
Crittenden, S. L. and Kimble, J. (2008). Analysis of the C. elegans germline stem cell region. *Methods Mol. Biol.* **450**, 27-44.
Crittenden, S. L., Bernstein, D. S., Bachorik, J. L., Thompson, B. E., Gallegos, M., Petcherski, A. G., Moulder, G., Barstead, R., Wickens, M. and Kimble, J. (2002). A conserved RNA-binding protein controls germline stem cells in Caenorhabditis elegans. *Nature* **417**, 660-663.
Crittenden, S. L., Leonhard, K. A., Byrd, D. T. and Kimble, J. (2006). Cellular analyses of the mitotic region in the Caenorhabditis elegans adult germ line. *Mol. Biol. Cell* **17**, 3051-3061.
Doronkin, S., Djagaeva, I. and Beckendorf, S. K. (2003). The COP9 signalosome promotes degradation of Cyclin E during early Drosophila oogenesis. *Dev. Cell* **4**, 699-710.
Doyle, T. G., Wen, C. and Greenwald, I. (2000). SEL-8, a nuclear protein required for LIN-12 and GLP-1 signaling in Caenorhabditis elegans. *Proc. Natl. Acad. Sci. USA* **97**, 7877-7881.
Drummond-Barbosa, D. and Spradling, A. C. (2001). Stem cells and their progeny respond to nutritional changes during Drosophila oogenesis. *Dev. Biol.* **231**, 265-278.
Eckmann, C. R., Crittenden, S. L., Suh, N. and Kimble, J. (2004). GLD-3 and control of the mitosis/meiosis decision in the germline of Caenorhabditis elegans. *Genetics* **168**, 147-160.
Fay, D. S. and Han, M. (2000). Mutations in cye-1, a Caenorhabditis elegans cyclin E homolog, reveal coordination between cell-cycle control and vulval development. *Development* **127**, 4049-4060.
Feng, H., Zhong, W., Punkosdy, G., Gu, S., Zhou, L., Seabolt, E. K. and Kipreos, E. T. (1999). CUL-2 is required for the G1-to-S-phase transition and mitotic chromosome condensation in Caenorhabditis elegans. *Nat. Cell Biol.* **1**, 486-492.
Francis, R., Maine, E. and Schedl, T. (1995). Analysis of the multiple roles of gld-1 in germline development: interactions with the sex determination cascade and the glp-1 signaling pathway. *Genetics* **139**, 607-630.
Fujita, M., Takeshita, H. and Sawa, H. (2007). Cyclin E and CDK2 repress the terminal differentiation of quiescent cells after asymmetric division in C. elegans. *PLoS ONE* **2**, e407.
Hansen, D. and Schedl, T. (2006). The regulatory network controlling the proliferation-meiotic entry decision in the Caenorhabditis elegans germ line. *Curr. Top. Dev. Biol.* **76**, 185-215.
Hansen, D., Hubbard, E. J. and Schedl, T. (2004a). Multi-pathway control of the proliferation versus meiotic development decision in the Caenorhabditis elegans germline. *Dev. Biol.* **268**, 342-357.
Hansen, D., Wilson-Berry, L., Dang, T. and Schedl, T. (2004b). Control of the proliferation versus meiotic development decision in the C. elegans germline through regulation of GLD-1 protein accumulation. *Development* **131**, 93-104.
Henderson, S. T., Gao, D., Lambie, E. J. and Kimble, J. (1994). lag-2 may encode a signaling ligand for the GLP-1 and LIN-12 receptors of C. elegans. *Development* **120**, 2913-2924.
Honigberg, S. M. and Purnapatre, K. (2003). Signal pathway integration in the switch from the mitotic cell cycle to meiosis in yeast. *J. Cell Sci.* **116**, 2137-2147.
Hsu, H. J., LaFever, L. and Drummond-Barbosa, D. (2008). Diet controls normal and tumorous germline stem cells via insulin-dependent and -independent mechanisms in Drosophila. *Dev. Biol.* **313**, 700-712.
Ito, K. and McGhee, J. D. (1987). Parental DNA strands segregate randomly during embryonic development of Caenorhabditis elegans. *Cell* **49**, 329-336.
Jantsch, V., Tang, L., Pasierbek, P., Penkner, A., Nayak, S., Baudrimont, A., Schedl, T., Gartner, A. and Loidl, J. (2007). Caenorhabditis elegans prom-1 is required for meiotic prophase progression and homologous chromosome pairing. *Mol. Biol. Cell* **18**, 4911-4920.
Jaramillo-Lambert, A., Ellefson, M., Villeneuve, A. M. and Engebrecht, J. (2007). Differential timing of S phases, X chromosome replication, and meiotic prophase in the C. elegans germ line. *Dev. Biol.* **308**, 206-221.
Jones, A. R. and Schedl, T. (1995). Mutations in gld-1, a female germ cell-specific tumor suppressor gene in Caenorhabditis elegans, affect a conserved domain also found in Src-associated protein Sam68. *Genes Dev.* **9**, 1491-1504.
Jones, A. R., Francis, R. and Schedl, T. (1996). GLD-1, a cytoplasmic protein essential for oocyte differentiation, shows stage- and sex-specific expression during Caenorhabditis elegans germline development. *Dev. Biol.* **180**, 165-183.
Kadyk, L. C. and Kimble, J. (1998). Genetic regulation of entry into meiosis in Caenorhabditis elegans. *Development* **125**, 1803-1813.
Kerins, J. A., Hanazawa, M., Dorsett, M. and Schedl, T. (2010). PRP-17 and the pre-mRNA splicing pathway are preferentially required for the proliferation versus meiotic development decision and germline sex determination in Caenorhabditis elegans. *Dev. Dyn.* **239**, 1555-1572.
Kim, J., Feng, H. and Kipreos, E. T. (2007). C. elegans CUL-4 prevents rereplication by promoting the nuclear export of CDC-6 via a CKI-1-dependent pathway. *Curr. Biol.* **17**, 966-972.
Kimble, J. and Crittenden, S. L. (2007). Controls of germline stem cells, entry into meiosis, and the sperm/oocyte decision in Caenorhabditis elegans. *Annu. Rev. Cell Dev. Biol.* **23**, 405-433.
Kipreos, E. T., Lander, L. E., Wing, J. P., He, W. W. and Hedgecock, E. M. (1996). cul-1 is required for cell cycle exit in C. elegans and identifies a novel gene family. *Cell* **85**, 829-839.
Lee, M. H., Ohmachi, M., Arur, S., Nayak, S., Francis, R., Church, D., Lambie, E. and Schedl, T. (2007). Multiple functions and dynamic activation of MPK-1 extracellular signal-regulated kinase signaling in Caenorhabditis elegans germline development. *Genetics* **177**, 2039-2062.
Lilly, M. A. and Spradling, A. C. (1996). The Drosophila endocycle is controlled by Cyclin E and lacks a checkpoint ensuring S-phase completion. *Genes Dev.* **10**, 2514-2526.
Maciejowski, J., Ugel, N., Mishra, B., Isopi, M. and Hubbard, E. J. (2006). Quantitative analysis of germline mitosis in adult C. elegans. *Dev. Biol.* **292**, 142-151.
Maine, E. M., Hansen, D., Springer, D. and Vought, V. E. (2004). Caenorhabditis elegans atx-2 promotes germline proliferation and the oocyte fate. *Genetics* **168**, 817-830.
Mantina, P., MacDonald, L., Kulaga, A., Zhao, L. and Hansen, D. (2009). A mutation in teg-4, which encodes a protein homologous to the SAP130 pre-mRNA splicing factor, disrupts the balance between proliferation and differentiation in the C. elegans germ line. *Mech. Dev.* **126**, 417-429.
Matson, C. K., Murphy, M. W., Griswold, M. D., Yoshida, S., Bardwell, V. J. and Zarkower, D. (2010). The mammalian doublesex homolog DMRT1 is a transcriptional gatekeeper that controls the mitosis versus meiosis decision in male germ cells. *Dev. Cell* **19**, 612-624.
Michaelson, D., Korta, D. Z., Capua, Y. and Hubbard, E. J. (2010). Insulin signaling promotes germline proliferation in C. elegans. *Development* **137**, 671-680.
Nadarajan, S., Govindan, J. A., McGovern, M., Hubbard, E. J. and Greenstein, D. (2009). MSP and GLP-1/Notch signaling coordinately regulate actomyosin-dependent cytoplasmic streaming and oocyte growth in C. elegans. *Development* **136**, 2223-2234.
Narbonne-Reveau, K. and Lilly, M. (2009). The Cyclin-dependent kinase inhibitor Dacapo promotes genomic stability during premeiotic S phase. *Mol. Biol. Cell* **20**, 1960-1969.
Nayak, S., Santiago, F. E., Jin, H., Lin, D., Schedl, T. and Kipreos, E. T. (2002). The Caenorhabditis elegans Skp1-related gene family: diverse functions in cell proliferation, morphogenesis, and meiosis. *Curr. Biol.* **12**, 277-287.
Neganova, I., Zhang, X., Atkinson, S. and Lako, M. (2009). Expression and functional analysis of G1 to S regulatory components reveals an important role for CDK2 in cell cycle regulation in human embryonic stem cells. *Oncogene* **28**, 20-30.
Orford, K. W. and Scadden, D. T. (2008). Deconstructing stem cell self-renewal: genetic insights into cell-cycle regulation. *Nat. Rev. Genet.* **9**, 115-128.
Park, M. and Krause, M. W. (1999). Regulation of postembryonic G(1) cell cycle progression in Caenorhabditis elegans by a cyclin D/CDK-like complex. *Development* **126**, 4849-4860.
Penkner, A. M., Fridkin, A., Gloggnitzer, J., Baudrimont, A., Machacek, T., Woglar, A., Csaszar, E., Pasierbek, P., Ammerer, G., Gruenbaum, Y. et al. (2009). Meiotic chromosome homology search involves modifications of the nuclear envelope protein Matefin/SUN-1. *Cell* **139**, 920-933.
Petcherski, A. G. and Kimble, J. (2000). LAG-3 is a putative transcriptional activator in the C. elegans Notch pathway. *Nature* **405**, 364-368.
Qiao, L., Lissemore, J. L., Shu, P., Smardon, A., Gelber, M. B. and Maine, E. M. (1995). Enhancers of glp-1, a gene required for cell-signaling in

Caenorhabditis elegans, define a set of genes required for germline development. *Genetics* **141**, 551-569.
Rempel, R. E., Sleight, S. B. and Maller, J. L. (1995). Maternal Xenopus Cdk2-cyclin E complexes function during meiotic and early embryonic cell cycles that lack a G1 phase. *J. Biol. Chem.* **270**, 6843-6855.
Richardson, H. E., O'Keefe, L. V., Reed, S. I. and Saint, R. (1993). A Drosophila G1-specific cyclin E homolog exhibits different modes of expression during embryogenesis. *Development* **119**, 673-690.
Rual, J. F., Ceron, J., Koreth, J., Hao, T., Nicot, A. S., Hirozane-Kishikawa, T., Vandenhaute, J., Orkin, S. H., Hill, D. E., van den Heuvel, S. et al. (2004). Toward improving Caenorhabditis elegans phenome mapping with an ORFeome-based RNAi library. *Genome Res.* **14**, 2162-2168.
Salic, A. and Mitchison, T. J. (2008). A chemical method for fast and sensitive detection of DNA synthesis in vivo. *Proc. Natl. Acad. Sci. USA* **105**, 2415-2420.
Sijen, T., Fleenor, J., Simmer, F., Thijssen, K. L., Parrish, S., Timmons, L., Plasterk, R. H. and Fire, A. (2001). On the role of RNA amplification in dsRNA-triggered gene silencing. *Cell* **107**, 465-476.
Stead, E., White, J., Faast, R., Conn, S., Goldstone, S., Rathjen, J., Dhingra, U., Rathjen, P., Walker, D. and Dalton, S. (2002). Pluripotent cell division cycles are driven by ectopic Cdk2, cyclin A/E and E2F activities. *Oncogene* **21**, 8320-8333.
Vought, V. E., Ohmachi, M., Lee, M. H. and Maine, E. M. (2005). EGO-1, a putative RNA-directed RNA polymerase, promotes germline proliferation in parallel with GLP-1/notch signaling and regulates the spatial organization of nuclear pore complexes and germline P granules in Caenorhabditis elegans. *Genetics* **170**, 1121-1132.
Wang, L., Eckmann, C. R., Kadyk, L. C., Wickens, M. and Kimble, J. (2002). A regulatory cytoplasmic poly(A) polymerase in Caenorhabditis elegans. *Nature* **419**, 312-316.
Wang, Z. A. and Kalderon, D. (2009). Cyclin E-dependent protein kinase activity regulates niche retention of Drosophila ovarian follicle stem cells. *Proc. Natl. Acad. Sci. USA* **106**, 21701-21706.
Wittenberg, C. and La Valle, R. (2003). Cell-cycle-regulatory elements and the control of cell differentiation in the budding yeast. *BioEssays* **25**, 856-867.
Zetka, M. C., Kawasaki, I., Strome, S. and Muller, F. (1999). Synapsis and chiasma formation in Caenorhabditis elegans require HIM-3, a meiotic chromosome core component that functions in chromosome segregation. *Genes Dev.* **13**, 2258-2270.